

Optimizing the Performance of Remote Phosphor LED

Yiting Zhu and Nadarajah Narendran

Lighting Research Center
Rensselaer Polytechnic Institute, Troy, NY 12180
www.lrc.rpi.edu

Zhu, Y. and N. Narendran. 2007. Optimizing the performance of remote phosphor LED. *Proceeding of First International Conference on White LEDs and Solid State Lighting*, Tokyo, Japan, November 26-30, 2007, P411–P414.

Copyright 2007. Illuminating Engineering Institute of Japan.

This paper is being distributed electronically under the “Fair Use Copyright Act.” One print or electronic copy may be made for personal use only. Systematic or multiple reproduction, distribution to multiple locations via electronic or other means, duplication of any material in this paper for a fee or for commercial purposes, or modification of the content of the paper are prohibited under United States and international laws.

Optimizing the Performance of Remote Phosphor LED

Yiting Zhu and Nadarajah Narendran

Lighting Research Center, Rensselaer Polytechnic Institute
21 Union Street, Troy, NY 12180, USA

ABSTRACT

The accuracy of results from Monte Carlo ray-tracing analysis significantly depends on the input values of the optical properties of the various package components. One important piece of input information is the phosphor particle MFP (mean-free-path), which is not easily determined. This study introduced a method to determine the MFP by matching the experimental results with optical ray-tracing analysis at a wavelength beyond the phosphor excitation range. Using these experiment values for MFP in an optical ray-tracing analysis of a white LED package showed an excellent match with measured results for light output and chromaticity.

1. INTRODUCTION

Presently, phosphor down-conversion is the dominant method for creating white light-emitting diodes (LEDs) [1-3]. Most commercial phosphor-converted (PC) white LEDs have followed the initial package design where the short-wavelength chip is surrounded by a phosphor layer [2]. During the past few years, the interest for remote phosphor LEDs—where the LED chip and the phosphor layer are physically separated—has been growing. The first remote phosphor LED configuration was proposed in 1995 [4]. Since then, several remote phosphor LED concepts have been proposed [5-7]. However, it was not until the middle of the present decade that the benefits of remote-phosphor LEDs were quantified [8,9]. These studies showed improved life and higher luminous efficacy for remote phosphor LEDs compared to traditional PC white LEDs [8,9]. In 2005, a method known as SPE (scattered photon extraction), in which the optics between the LED chip and the remote phosphor layer are tailored to extract the backscattered light from the phosphor layer, experimentally showed as much as 60% improvement in light output and luminous efficacy [9]. Since 2005, a growing number of publications have documented

investigations of remote phosphor LEDs [10-13]. Many of these studies used optical ray-tracing analysis to investigate performance improvements of remote phosphor LEDs [10,11]. Some of the popular optical ray-tracing packages use the Monte Carlo method for their algorithm. Even though optical ray-tracing analysis is a very popular tool amongst the optics community, the accuracy of the results depends on the assumptions and input values for the optical properties of each component in the package. In some past studies, the experimental results showed large discrepancies from the optical ray-tracing analysis results. These discrepancies most likely arose as a result of incorrect assumptions for the optical properties of commonly used phosphors, such as their transmission and reflection values. Generally, the phosphors commonly used in PC white LEDs behave like a scattering medium, with a greater proportion of light converted by the phosphor sent back toward the LED chip [14].

One of the challenges in conducting ray-tracing analysis is not knowing the accurate value for the mean-free-path (MFP) of the phosphor particles in the medium. MFP denotes the average distance that the photon travels between collisions with phosphor particles [15]. MFP depends on phosphor particle size and phosphor density in the mixture. In reality, there are many factors that can affect the accuracy of the MFP value, such as particle agglomerations and the uniformity of the phosphor particle distribution within the phosphor-encapsulant mixture. Any inaccuracies in the estimation of the MFP value will result in incorrect results. Therefore, it is essential that the phosphor medium used in a ray-tracing analysis be characterized first and the MFP be determined.

The objective of the study presented in this paper was to analyze a remote phosphor white LED package with scattered photon extraction (SPE) using optical ray-tracing and compare the results to experimentally obtained values. Since the MFP value is unknown, we created several phosphor samples and measured their light transmission and reflection properties. Then the

MFP values of the different phosphor samples were determined by matching these experiment results to the ray-tracing analysis results.

2. EXPERIMENT

Optical Properties of Phosphor Layer

Four total internal reflection (TIR) optical lenses were coated with YAG:Ce phosphor of different area densities. The thickness of the phosphor coatings were kept constant. The area densities of the phosphor-encapsulant coatings were 4, 6, 8, and 10 mg/cm². The phosphor-coated TIR lens was mounted on top of a high-power LED. Two types of LEDs, a blue and a red, were used in the experiment. The blue LED had a peak wavelength of 465 nm and the red had a peak wavelength of 625 nm. The blue LED spectrum was within the excitation range of the YAG:Ce phosphor, but the red LED spectrum was outside the excitation range. Because the spectrum for blue light was within the phosphor excitation wavelength range, part of the blue light would be absorbed and converted into a broadband longer wavelength light and would be emitted in all directions. However, the red light, which had a spectrum outside the phosphor excitation wavelength range, would only be scattered by the phosphor.

The total light output for the blue and red LEDs were first measured in an integrating sphere with a clear TIR lens (without any phosphor-encapsulant coating) on top of the LEDs. This provided the total light emitted by these LEDs. Next, the LED-TIR lens combinations were placed inside an integrating sphere, one at a time, and the forward transmitted and backward reflected light from the phosphor layer were measured. The light output in the forward direction was measured by blocking the light emitted to the side and the back. Since the total and the forward light were measured, the light emitted in the backward direction was calculated. Therefore, the forward and backward ratios of the total light output for the two LEDs at the different phosphor area densities were calculated. In addition to the flux measurements, the chromaticity values were also recorded at each measurement.

MFP determination

LightTools™ 5.3.0 was used in this ray-tracing analysis. We input to the simulation the geometrical size of each component, the excitation, emission, and absorption spectra of the YAG:Ce phosphor used in the experiment and the transmission and reflection properties of the phosphor samples. The MFP describes the phosphor density in the phosphor-encapsulant mixture. Using the experiment results from the previous section from the red LED and matching the ratios of transmitted radiant energy (or reflected) and overall radiant energy, we estimated the corresponding MFP values for the different phosphor layers used in this study. Then the same MFP value was used with the blue LED to obtain accurate results for white light.

White light source analysis

A ray-tracing analysis for an SPE remote phosphor package [9], as shown in Fig.1(a), was conducted. Both the overall and the forward transmitted light output through the secondary optics and their corresponding chromaticity coordinates were calculated. The blue LED light source and the four TIR lenses with different phosphor area densities were simulated. The MFP values obtained from the previous section with the red LED were used in this optical ray-tracing analysis. The results for light output and chromaticity from ray-tracing analysis and laboratory measurements are shown in Fig. 2 and Fig. 3. As seen in these figures, the ray-tracing analysis results and laboratory experiment results matched very well.

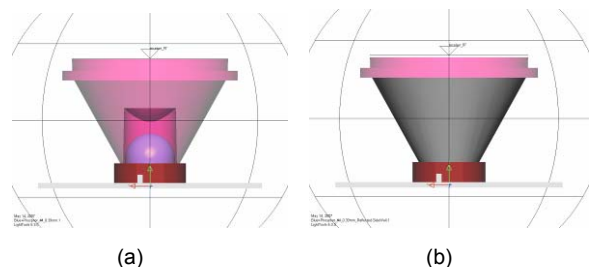
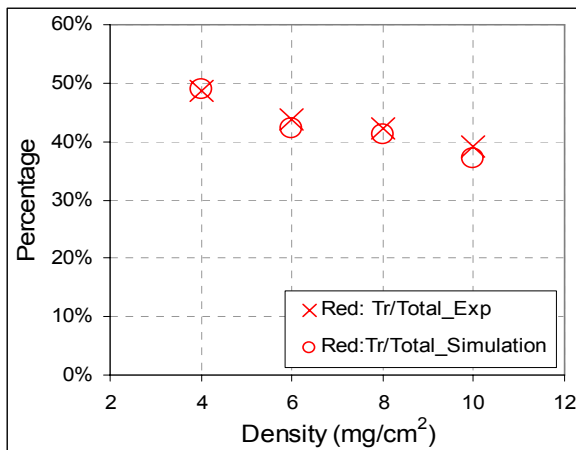
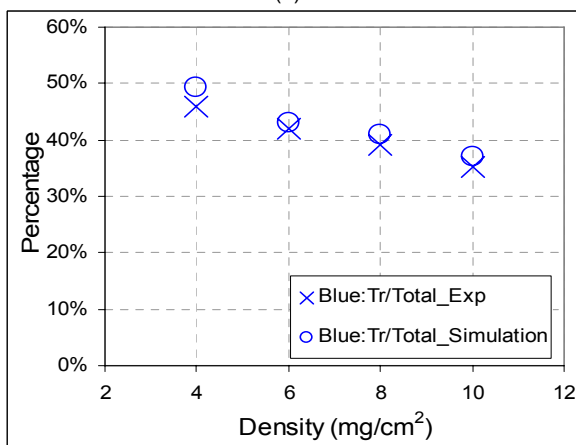


Fig. 1: (a) SPE package with transparent side wall surfaces; (b) remote phosphor package with reflective side wall surfaces.



(a)



(b)

Fig. 2: (a) The simulated result matched the experimental result in determining the MFP values of red light impinging on the secondary optics in an SPE package. (b) The simulated result verified the experimental result for the blue light impinging on the secondary optics in an SPE package.

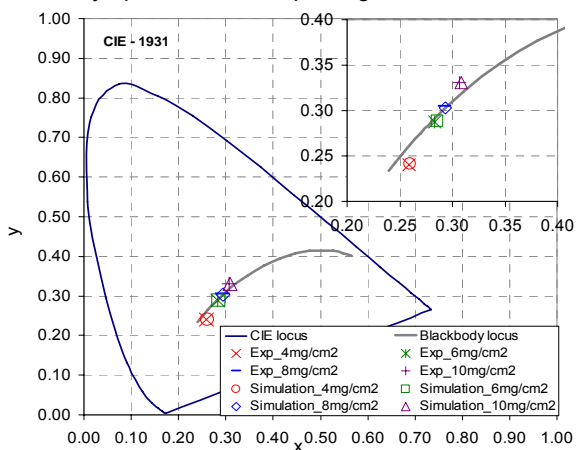


Fig. 3 The simulated result verified the experimental result for the chromaticity coordinates in the blue light SPE package.

Next, two types of remote phosphor SPE packages, illustrated in Fig. 1(a) and Fig. 1(b), were analyzed using optical ray-tracing. Here, one is the SPE package with transparent secondary optics to extract backscattering light through the side walls; the other is the same package with reflective side walls, which reflects the backscattered light out of the package through the top surface. Reflective side wall packages were simulated with reflectances ranging from 35% to 95%. The results are shown in Fig. 4. The chromaticity values for the packages with reflective side walls shifted to yellow when the side wall reflectances increased, along with increasing luminous output. Comparing these results to the SPE package with transparent side walls and a phosphor area density of 8 mg/cm², which produced chromaticity coordinates located on the blackbody curve of the CIE 1931 color chart, showed that the chromaticity coordinates of the SPE package were close to those of the reflective side wall packages with 75% and 85% reflectances, as shown in Fig. 4. With similar chromaticity coordinates, the SPE package with transparent side walls was proved to have 30% to 40% higher light output than the SPE package with reflective side surfaces, as shown in Fig. 5.

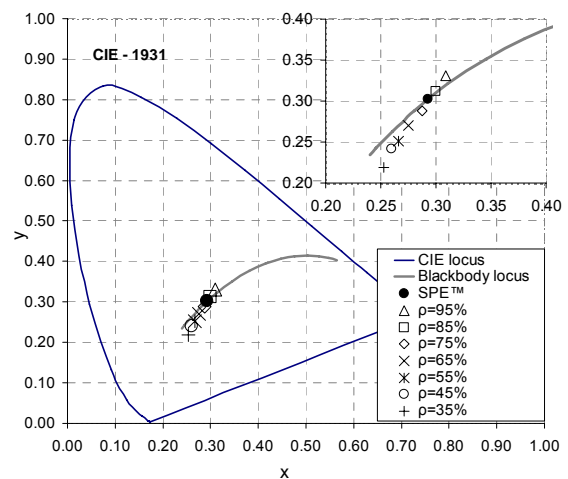


Fig. 4 Chromaticity coordinates of the SPE package with transparent side surfaces compared with the remote phosphor package with reflective side surfaces with reflectances from 35% to 95%.

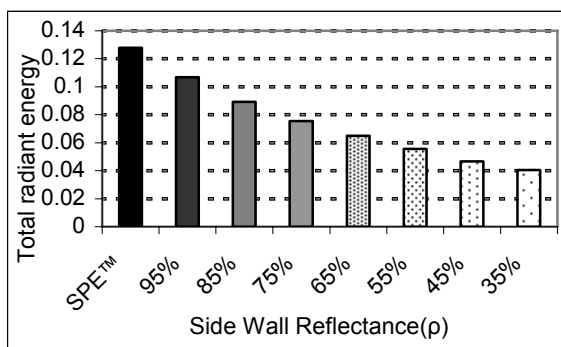


Fig. 5. Total light output comparison of SPE with transparent side wall surfaces against remote phosphor packages with reflective side surfaces with 35% to 95% reflectance.

3. CONCLUSIONS

Characterizing the phosphor layers with a light source outside the excitation range and determining the MFP for optical ray-tracing analysis provided an excellent match between optical ray-tracing analysis results and experiment results for light output and chromaticity. Additional optical ray-tracing analysis of SPE packages with transparent and reflective sides showed that transparent side SPE provides higher light output. However, one has to note that for directional lighting applications, additional reflectors are needed to redirect the side wall extracted light. In such cases, the difference between the two configurations may be lower.

ACKNOWLEDGEMENTS

Our special thanks go to Jennifer Taylor for editing this paper, to Yimin Gu and Jean Paul Freyssonier for giving very valuable suggestions, and to Applied NanoWorks for supplying the facilities for some of the measurements.

REFERENCES

- [1] K. Bando, Y. Noguchi, Y., K. Sakano, and Y. Shimizu, Tech. Digest, Phosphor Res. Soc. 264th Meeting, 5-14 (1996).
- [2] S. Nakamura and G. Fasol, *The Blue Laser Diode: GaN Based Light Emitters and Lasers*, Berlin: Springer (1997).

- [3] R. Mueller-Mach, G. Mueller, M. Krames, T. Trottier, *IEEE J. Sel. Topics Quantum Electron.*, 8(2) (2002) 339-345.
- [4] T. Abe, US Patent 5,535,230, Jan. 3, 1995.
- [5] H. Chen, US Patent 5,962,971, Aug. 29, 1997.
- [6] C. H. Lowery, US Patent 5,959,316, Sept. 1, 1998.
- [7] A. Duggal, et al., US Patent 6,294,800 B1, Nov. 30, 1998.
- [8] N. Narendran, Y. Gu, J.P. Freyssonier, H. Yu, L. Deng, *J. Crystal Growth* 268 (2004) 449-245.
- [9] N. Narendran, Y. Gu, J. Freyssonier-Nova, Y. Zhu, *Phys. Stat. Sol.(a)* 202(6) (2005) R60-R62.
- [10] H. Luo, J. Kim, E. Schubert, J. Cho, C. Sone, Y. Park, *Appl. Phys. Lett.* 86 (2005) 243505.
- [11] B. Parkyn, J. Chaves and W. Falicoff, *Proc. of SPIE*, 5942 (2005) 59420M.
- [12] H. Masui, S. Nakamura, S. DenBaars, *Jpn. J. Appl. Phys.* 45(34) (2006) L910-L912.
- [13] S. Bierhuizen, M. Krames, G. Harbers, G. Weijers, *Proc. of SPIE* 6669 (2007) 66690B.
- [14] Y. Zhu, N. Narendran, Y. Gu, *Proc. of SPIE*, 6337 (2006) 63370S.
- [15] C. Kittel. *Introduction to Solid State Physic*, John Wiley & Sons, Inc (2005).